8230 *Inorg. Chem.* **2010**, *49*, 8230–8236
DOI: 10.1021/ic100273q

Inorganic Chemistry
Article

Correlation between Structural and Semiconductor−Metal Changes and Extreme Conditions Materials Chemistry in Ge−Sn

Christophe L. Guillaume,[†,⊗] George Serghiou,[*,†] Andrew Thomson,[†,○] Jean-Paul Morniroli,[‡] Dan J. Frost,[§] Nicholas Odling,[∥] and Chris E. Jeffree[⊥]

[†]*School of Engineering and Centre for Materials Science, University of Edinburgh, Kings Buildings, Mayfield Road, Edinburgh EH9 3JL, U.K.,* [‡]*Laboratoire de Métallurgie Physique et Génie des Matériaux, UMR CNRS 8517, Université des Sciences et Technologies de Lille et Ecole Nationale Supérieure de Chimie de Lille, Cité Scientifique, 59655 Villeneuve d'Ascq Cedex, France,* [§]*Bayerisches Geoinstitut, Universität Bayreuth, D-95440, Bayreuth Germany,* [∥]*School of Geosciences, The Grant Institute, University of Edinburgh, Kings Buildings, West Mains Road, Edinburgh EH9 3JW, U.K., and* [⊥]*School of Biological Sciences, Michael Swann Building, University of Edinburgh, Kings Buildings, Mayfield Road, Edinburgh EH9 3JR, U.K.* [⊗] *Present address: School of Physics, University of Edinburgh, Mayfield Road, Edinburgh EH9 3JL, U.K.* [○] *Present address: BP Chemicals Ltd, Saltend, Hedon, Hull, HU12 8DS, U.K.*

Received February 9, 2010

High pressure and temperature experiments on Ge−Sn mixtures to 24 GPa and 2000 K reveal segregation of Sn from Ge below 10 GPa whereas Ge−Sn agglomerates persist above 10 GPa regardless of heat treatment. At 10 GPa Ge reacts with Sn to form a tetragonal $P4_32_12$ $Ge_{0.9}Sn_{0.1}$ solid solution on recovery, of interest for optoelectronic applications. Using electron diffraction and scanning electron microscopy measurements in conjunction with a series of tailored experiments promoting equilibrium and kinetically hindered synthetic conditions, we provide a step by step correlation between the semiconductor−metal and structural changes of the solid and liquid states of the two elements, and whether they segregate, mix or react upon compression. We identify depletion zones as an effective monitor for whether the process is moving toward reaction or segregation. This work hence also serves as a reference for interpretation of complex agglomerates and for developing successful synthesis conditions for new materials using extremes of pressure and temperature.

Introduction

Any recovered solid state product from any synthesis will be either segregated, reacted, or mixed or a combination of these states. Indeed, a longstanding challenge for successful synthesis has been to understand and control which state will form, based on synthetic conditions and the structural and electronic characteristics of the starting materials. To do this, it is very important to be able to interpret and correlate the frequently complex synthetic agglomerates, with both the synthesis conditions and the starting material characteristics, to channel the next experiment in the right direction. High pressure offers a powerful means by which to modify the structural and electronic characteristics of the starting materials and in conjunction with temperature to generate a range of synthetic conditions. Indeed, our ability to make new materials can be profoundly enhanced using pressure and temperature to overcome ambient condition constraints to synthesis. We have recently demonstrated this by preparing a Ge−Sn crystalline solid solution near 10 GPa[1] of optoelectronic importance,[1,2] whereas no mutual bulk solubility exists between the two at ambient pressure.[3] Ge is a semiconductor at ambient pressure with the cubic diamond structure.[4] Above about 10 GPa it undergoes a phase transition to the tetragonal β-Sn structure ($I4_1/amd$)[5,6] (and references therein). High pressure and temperature phase relations in this system have been documented up to 11 GPa and 950 K, and its melting curve has been determined to 40 GPa.[5,7,8] The local structure of liquid Ge is reported with

*To whom correspondence should be addressed. E-mail: george.serghiou@ed.ac.uk.

(1) Guillaume, C.; Serghiou, G.; Thomson, A.; Morniroli, J. P.; Frost, D. J.; Odling, N.; Mezouar, M. *J. Am. Chem. Soc.* **2009**, *131*, 7550–7551.
(2) Serghiou, G.; Guillaume, C. L.; Jeffree, C. E.; Thomson, A.; Frost, D. J.; Morniroli, J. P.; Odling, N. *High Pressure Res.* **2010**, *30*, 44–50.
(3) Massalski, T. *Binary Alloy Phase diagrams*, 2nd ed.; ASM International: Materials Park, OH, 1990; Vol. *2*.
(4) Schackelford, J. F. *Introduction to Materials Science for Engineers*, 5th ed.; Prentice Hall: New York, 1999.
(5) Young, D. A. *Phase Diagrams of the Elements*, 1st ed.; University of California Press: Berkeley, CA, 1991.
(6) Ackland, G. J. *Rep. Prog. Phys.* **2001**, *64*, 483–516.
(7) Voronin, G. A.; Pantea, C.; Zerda, T. W.; Zhang, J.; Wang, L.; Zhao, Y. *J. Phys. Chem. Solids* **2005**, *64*, 2113–2119.
(8) Prakapenka, V.; Kubo, A.; Kuznetsov, A.; Laskin, A.; Shkurikhin, O.; Dera, P.; Rivers, M. L.; Sutton, S. R. *High Pressure Res.* **2008**, *28*, 225–235.

 Published on Web 08/16/2010

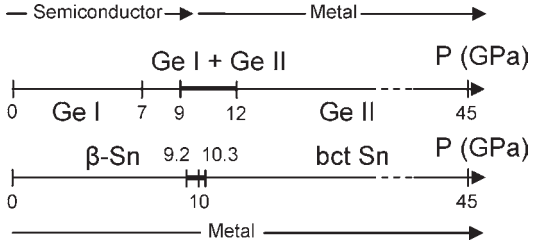

Figure 1. Crystal structure comparison of Ge and Sn upon room temperature compression, to 45 GPa. Semiconducting GeI (cubic diamond structure) transforms to metallic GeII (β-Sn structure ($I4_1/amd$)) above about 9 GPa and coexists with GeII to 12 GPa.[7] GeII can be retained to about 7 GPa upon decompression.[7] There is a smaller region near 10 GPa where the metal−metal transition from β-Sn ($I4_1/amd$) to bct Sn ($I4/mmm$) occurs (9.2−10.3 GPa).[5,12].

increasing pressure to transform from a disordered β-tin structure with mixed covalent and metallic bonding to an ordered β-Sn structure with increasing metallic character.[9−11] At ambient pressure, Sn has the diamond structure (α-Sn) below 291 K and adopts the β-Sn structure ($I4_1/amd$) above 291 K. β-Sn undergoes a transition to a body centered tetragonal structure (bct, $I4/mmm$) at about 10 GPa, which is stable to 45 GPa.[6,12] High pressure and temperature phase relations for the tin system have been measured up to 16 GPa and 420 K, and the melting curve of tin has been determined up to 20 GPa.[11,13,14] No other tin phases were found in this region, and the transformations are reversible. At between 9 and 10 GPa, upon compression, Ge and Sn can adopt the same crystal structure (β-Sn) (Figure 1), and their atomic radii ratios are then within 13% of each other, whereas in all other cases at, or above room temperature compression, their atomic radii ratios differ by 20% or more (the ratio decreases to 20% at 24 GPa).[1,12,13,15−17] Further, the nominal valencies and electronegativities of the two elements are similar above 9 GPa when they are both in the metallic state.[18−22] Thus the Hume−Rothery criteria (i, atomic radii difference $< 15\%$; ii, similar electronegativities; iii, same crystal structure; iv, same valence)[5,23] upon compression are most closely satisfied near 10 GPa. Studies of the liquid states of Ge and Sn reveal that existing structural and electronic similarity of the two at ambient pressure is enhanced with pressure with the higher

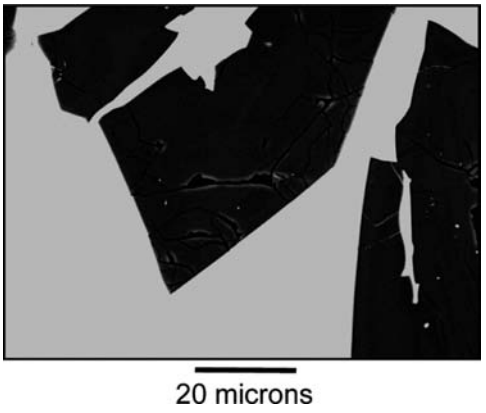

Figure 2. SEM image in BSE (Backscattered Electron) mode of a polished section of the capsule of a Ge−Sn sample quenched from 1500 K after heating for 5 min at 3 GPa. Semiquantitative results from numerous EDX analyses of the two regions reveal segregation of Sn (light contrast regions) from Ge (dark contrast regions).

pressure structural and electronic character of Ge liquid increasingly resembling that which liquid Sn already exhibits at ambient pressure.[9−11,24] The similarity between liquid Ge and Sn at ambient pressure is significant enough that a single binary liquid phase already occurs at ambient pressure, but the tendency for segregation in the liquid state increases markedly with decreasing temperature.[3,25] As first shown by Predel for binary liquid alloys,[26] the tendency for segregation will decrease with increasing pressure as Ge and Sn become more similar.

Here, we succeed in capturing, with an unprecedented detail needed, the evolution from segregation to reactivity to mixing in the Ge−Sn system upon compression, to be able to correlate these transformations directly, with the electronic and structural transformations of Ge and Sn in their solid and liquid states. For this we employ a range of vessels from 1 atm furnaces to high pressure piston cylinder and multianvil devices. These are coupled with electron microscopy analysis which allows us to visualize the chemical, morphological, and structural changes within the Ge−Sn system with highest spatial resolution for a range of tailored experiments promoting, instrumentally, both equilibrium and kinetically hindered conditions.

Experimental Section

We employ ultrapure Ge (99.9999+% puratronic Alfa Aesar) and Sn ($I4_1/amd$) (99.999 metal basis % Alfa Aesar) starting materials. For the ambient pressure experiments equimolar Ge and Sn samples were heated at 1500 K in a 90% Ar −10% H_2 atmosphere for up to 120 min and temperature quenched. Compositions ranging from equimolar to 3:1 Ge to Sn in several piston cylinder experiments were heated at 1500 K for up to 120 min and up to 3.5 GPa followed by temperature and pressure quenching. Twenty multianvil experiments on samples ranging from endmember to equimolar, 3:1 or 6:1 Ge to Sn mixtures were performed at pressures ranging from 7 to 24 GPa and temperatures to 2000 K for up to 30 min heating duration, followed by either quenching or annealing at lower temperatures up to 1050 K

(9) Tsuji, K.; Hattori, T.; Mori, T.; Kinoshita, T.; Narushima, T.; Funamori, N. *J. Phys.: Condens. Matter* **2004**, *16*, 989–996.
(10) Koga, J.; Okumura, H.; Nishio, K.; Yamaguchi, T.; Yonezawa, F. *Phys. Rev. B* **2002**, *66*, 064211–064220.
(11) Narushima, T.; Hattori, T.; Kinoshita, T.; Hinzmann, A.; Tsuji, K. *Phys. Rev. B* **2007**, *76*, 104204.
(12) Liu, M.; Liu, L.-G. *High Temp.-High Pressures* **1986**, *18*, 79–85.
(13) Plymate, T. G.; Stout, J. H.; Cavaleri, M. E. *J. Phys. Chem. Solids* **1988**, *49*, 1339–1348.
(14) Cavaleri, M. E.; Plymate, T. G.; Scout, J. H. *J. Phys. Chem. Solids* **1988**, 945–956.
(15) Di Cicco, A.; Frasini, A. C.; Minicucci, M.; Principi, E.; Itie, J. P.; Munsch, P. *Phys. Status Solidi B* **2003**, *240*, 19–28.
(16) Chang, K. J.; Cohen, M. L. *Phys. Rev. B* **1986**, *34*, 8581–8590.
(17) Thewlis, J.; Davey, A. R. *Nature* **1954**, *174*, 1011–1011.
(18) Pearson, W. B. *The Crystal Chemistry and Physics of Metals and Alloys*, 2nd ed.; Wiley-Interscience: Chichester, 1972.
(19) Pauling, L. *The Nature of the Chemical Bond*; Cornell University Press: New York, 1960.
(20) Pauling, L.; Pauling, P. *Acta Crystallogr.* **1956**, *9*, 127–130.
(21) Shriver, D. F.; Atkins, P. W. *Inorganic Chemistry*; Oxford University Press: Oxford, 1999.
(22) Housecroft, C. E.; Sharpe, A. G. *Inorganic Chemistry*; Pearson Education Limited: New York, 2005.
(23) Hume-Rothery, W.; Smallman, R. E.; Haworth, C. W. *The Structure of Metals and Alloys*, 5th ed.; The Chaucer Press: London, 1969.
(24) Itami, T.; Munejiri, S.; Masaki, T.; Aoki, H.; Ishii, Y.; Kamiyama, T.; Senda, Y.; Shimojo, F.; Hoshino, K. *Phys. Rev. B* **2003**, *67*, 064201–0642212.
(25) Goto, R.; Shimojo, F.; Munejiri, S.; Hoshino, K. *J. Phys. Soc. Jpn.* **2004**, *73*, 2746–2752.
(26) Predel, B. *Acta Metallurgica* **1966**, *14*, 209–219.

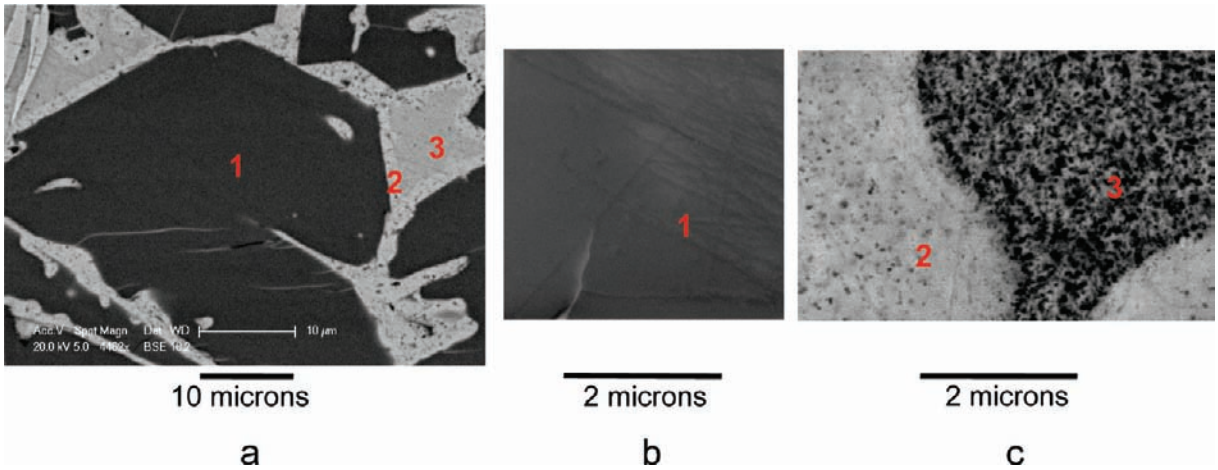

Figure 3. (a) SEM image in BSE mode of a polished section of the capsule of a Ge−Sn sample quenched from 1500 K after heating for 10 min at 7 GPa. Numerous EDX analyses from the three different contrast regions reveal virtually pure Ge in the darkest region (1), as well as two lighter contrast regions containing agglomerates of Ge−Sn, with the brightest contrast regions (2) (depletion zone), containing about 14 at% less Ge than the intermediate contrast regions (3). Higher resolution field emission gun scanning electron microscopy images of the (b) darkest contrast pure Ge region (1) revealing its chemical homogeneity is also shown, as are images of the (c) brightest (2) and intermediate (3) contrast regions revealing even more clearly the pronounced chemical heterogeneity in these regions (see also Supporting Information).

and annealing times up to 5 h. Temperatures in the ambient and piston cylinder experiments were measured with Pt/$Pt_{87}Rh_{13}$ thermocouples and in the multianvil experiments with $W_{75}Re_{25}/W_{97}Re_3$ thermocouples, with emf's uncorrected for pressure. Pressure calibrations were performed with a variety of assemblies using a number of high pressure ambient and high pressure−high temperature phase transformations. These are discussed in previous work.[27−30] Further details and tabulations of the experimental runs can be found in section I of the Supporting Information.

Scanning Electron Microscopy (Philips XL30CP, with an energy dispersive X-ray analyzer (Oxford instruments EDX detector − SiLi crystal with PGT spirit analysis software) as well as Field Emission Gun Scanning Electron Microscopy (Hitachi S-4700 type II cold FEG SEM equipped with an EDAX Phoenix X-ray microanalysis system [SiLi crystal detector] and an Yttrium−Aluminum-Garnet [YAG] scintillator BSE detector) were employed for chemical and morphological analysis. The spatial resolution afforded by a FEGSEM is typically, in our measurements, about an order of magnitude higher than that of a SEM. The acceleration voltages used were 10 kV and 20 kV in backscattered electron mode for adjustable chemical contrast.[31] Secondary electrons were also used to differentiate between chemical and morphological heterogeneity. Further details on compositional and morphological analysis and tabulations of the experimental results described below are found in section II of the Supporting Information. Moreover, definition of salient terminology used here, is presented in section III of the Supporting Information. Samples were also investigated with a Philips CM30, Transmission Electron Microscope (TEM), equipped with a Gatan slow scan CCD camera and with Digital Micrograph software for acquisition of electron diffraction patterns and bright-field imaging with an accelerating voltage of 300 kV. The CM30 is also equipped with an EDX detector for further chemical analysis. This additional highest resolution (∼5 nm) chemical analysis was performed in spot, line scan or mapping mode in Scanning Transmission Electron Microscope (STEM) mode. Both convergent beam, precession electron diffraction, and microdiffraction (electron diffraction with a nearly parallel incident beam focused on the specimen with a small spotsize in the range 10 to 50 nm) were used for collecting diffraction patterns.[32−34]

Results

Recovered samples from experiments up to 9 GPa all show separation of Sn from Ge up to this pressure, either directly upon melt-quenching (ambient to 3.5 GPa) (Figure 2) or after annealing (7−9 GPa) (Figures 3−6). In particular, up to 3.5 GPa, direct quenching from the melt results in segregation of Sn from Ge and the boundaries between Ge and Sn are sharp, with no compositional gradient at the Ge rims (Figure 2). At 7 GPa direct quenching from the melt results in a pure Ge phase and a two phase Sn- rich region composed of a core agglomerate containing twice as much Ge as the lighter contrast Ge−Sn agglomerate situated adjacent to the pure Ge phase (Figure 3). At 8 GPa the starting mix was annealed at 820 K after melt-quenching. A residual melt-quenched region, however, is recovered together with the bulk subsolidus annealed product (Figure 4). In the subsolidus annealed product, Sn is segregated from Ge and there is no compositional gradient adjacent to the pure Ge phase (darkest contrast) (Figure 4b). Contrastingly, the Ge-rich agglomerate (intermediate contrast region) in the melt-quenched region is drastically depleted in the area adjacent to the pure Ge phase in the subsolidus region (Figure 4b). At 9 GPa direct quenching from the melt results in an intimate mixture of Ge and Sn-rich agglomerates (Figure 5). This increasing difficulty in separating Sn from Ge at 9 GPa, even as compared to proximal 7 or 8 GPa, as the tendency for segregation in the liquid state decreases further, and the metallic character of the solid states converge, can be seen by the nature of the reaction products in a further experiment at

(27) Keppler, H.; Frost, D. J. *EMU Notes in Mineralogy* **2005**, *7*, 1–30.
(28) Rubie, D. C. *Phase Transitions* **1999**, *68*, 431–451.
(29) Frost, D. J.; Poe, B. T.; Tronnes, R. G.; Liebske, C.; Duba, A.; Rubie, D. C. *Phys. Earth Planet. Inter.* **2004**, *143−144*, 507–514.
(30) van Westrenen, W.; Van Orman, J. A.; Watson, H.; Fei, Y.; Bruce Watson, E. *Geochem., Geophys., Geosyst.* **2003**, *4*, 1–10.
(31) Goldstein, J. I.; Newbury, D. E.; Echlin, P. *Scanning Electron Microscopy and X-ray Microanalysis*; Plenum Press: New York, 1992.
(32) Morniroli, J. P.; No, M. L.; Rodriguez, P. P.; San Juan, J.; Jezierska, E.; Michel, N.; Poulat, S.; Priester, L. *Ultramicroscopy* **2003**, *98*, 9–26.
(33) Holmestad, R.; Morniroli, J. P.; Zuo, J. M.; Spence, J. C. H.; Avilov, A. *Electron Microsc.* **1997**, *153*, 137–140.
(34) Williams, D. B.; Barry Carter, C. *Transmission Electron Microscopy*, 1st ed; Plenum Press: New York, 1996.

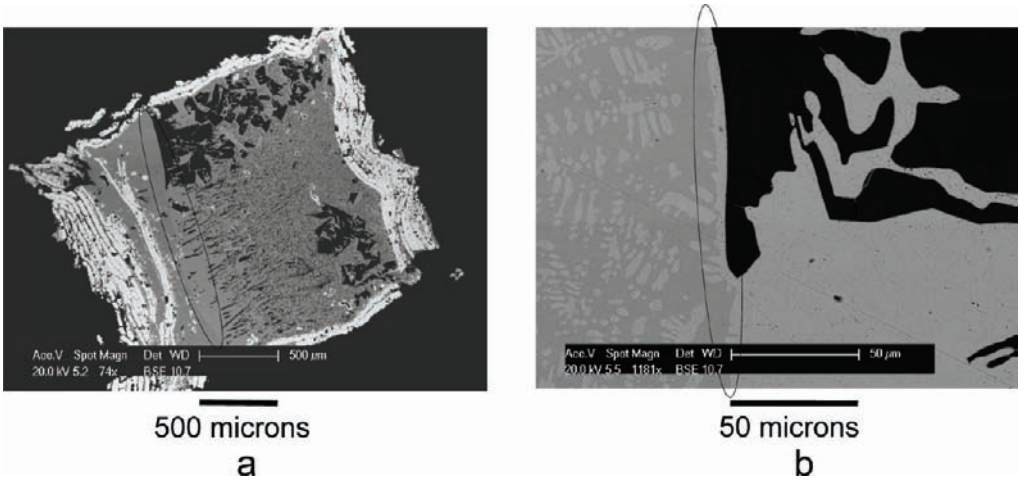

Figure 4. Lower (a) and higher (b) magnification SEM images in BSE mode of a polished section of the capsule of a Ge−Sn sample heated at 1500 K at 8 GPa for 5 min followed by annealing at 820 K for 1 h before quenching. The part of the image to the left of the boundary in (a) and (b) is quenched directly from the melt, possibly because of a thermal[35] or density gradient. The boundary is circled in (a) and (b). Numerous EDX analyses from the three different contrast regions shown in higher magnification in (b) reveal virtually pure Ge in the darkest regions, and about 20 at% less Ge in the brightest contrast regions than in the intermediate contrast Ge−Sn agglomerate. The very bright contrast region in (a) surrounding the reaction product is the rhenium capsule (see also Supporting Information).

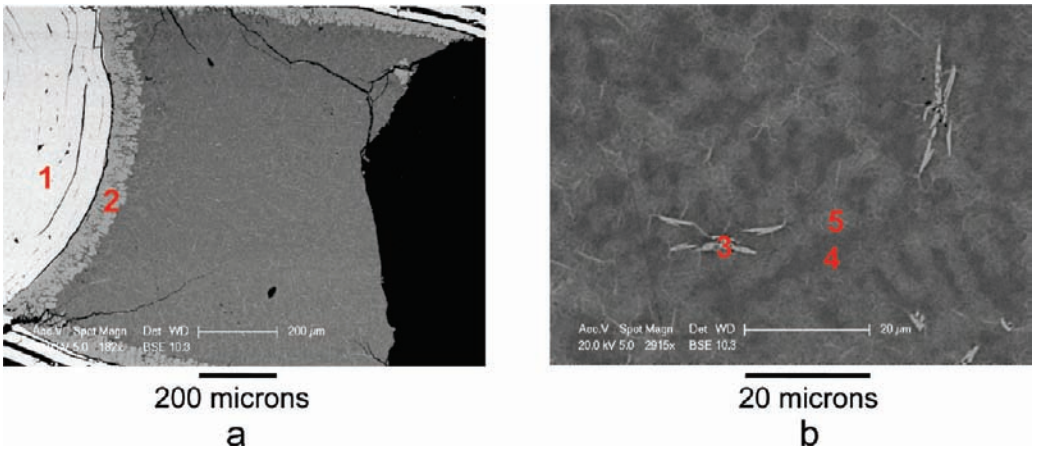

Figure 5. Lower (a) and higher (b) magnification SEM images in BSE mode of a polished section of the capsule of a Ge−Sn sample quenched from 1500 K after heating for 5 min at 9 GPa. Numerous EDX analyses from the five different contrast regions as labeled in the figures show that the brightest contrast region is the rhenium capsule (1), the somewhat lighter contrast region is a Re−Ge phase (2), the needles correspond to a Re−Ge phase or Re−Ge−Sn phase (3), and the darker and lighter colored regions in the interior are Ge−Sn agglomerates, with the darker region (4) containing about 12 at% more Ge than the lighter contrast region (5) (see also Supporting Information).

9 GPa where the sample was annealed at 1000 K after melting (Figure 6). This temperature is close to the liquidus,[5] and indeed the majority of the recovered product is quenched from the melt (Figure 6) and resembles the intimate mixture of Ge and Sn-rich agglomerates shown in Figure 5. The cooler upper and lower rims of the capsule, however, allow subsolidus annealing of the mixture near the rims, giving rise to pure Ge and a two phase Sn-rich region, with the area adjacent to pure Ge being Sn richer (Figure 6c). These observations again designate that segregation of the two components is not yet complete upon quenching from 1000 K (and from somewhat lower temperature near the rims), and that reaction between Ge and Sn is not favored at this pressure either. The situation is drastically changed at 10 GPa where after melt-quenching and subsequent annealing at 770 K, a region with a uniform $Ge_{0.9}Sn_{0.1}$ composition, uniquely spanning almost the entire capsule is obtained, with a residual melt-quenched product being recovered as well (Figure 7).

Extensive EDX measurements in SEM and STEM mode reveal a uniform $Ge_{0.9}Sn_{0.1}$ composition. No elemental germanium or tin was detected anywhere.[1] Zone-axis diffraction patterns from numerous crystals throughout the homogeneous chemically analyzed region were collected, two of which are shown in Figure 8. The program electron diffraction version 7.01[36] was used to interpret the zone-axis microdiffraction patterns. These showed excellent fits to the $P4_32_12$ tetragonal structure of Ge, which combined with a supporting angular diffraction pattern give lattice parameters (a = 6.014 (1) Å, c = 7.057 (1) Å, Z = 12)[1,37] which are greater with respect to end-member tetragonal Ge by 1.4 and 1.1% because of incorporation of the larger Sn atoms in the structure. The density of tetragonal $Ge_{0.9}Sn_{0.1}$ is ρ = 6.028 g/cm^3, making it 2.2% denser

(35) Schmidt, M. W.; Ulmer, P. *Geochim. Cosmochim. Acta* **2004**, *68*, 1889–1899.
(36) Morniroli, J. P. *Electron Diffraction*, 7.01; LMPGM UMR CNRS 8517: France, 2004.
(37) Kasper, J. S.; Richards, S. M. *Acta Crystallogr.* **1964**, *17*, 752–755.

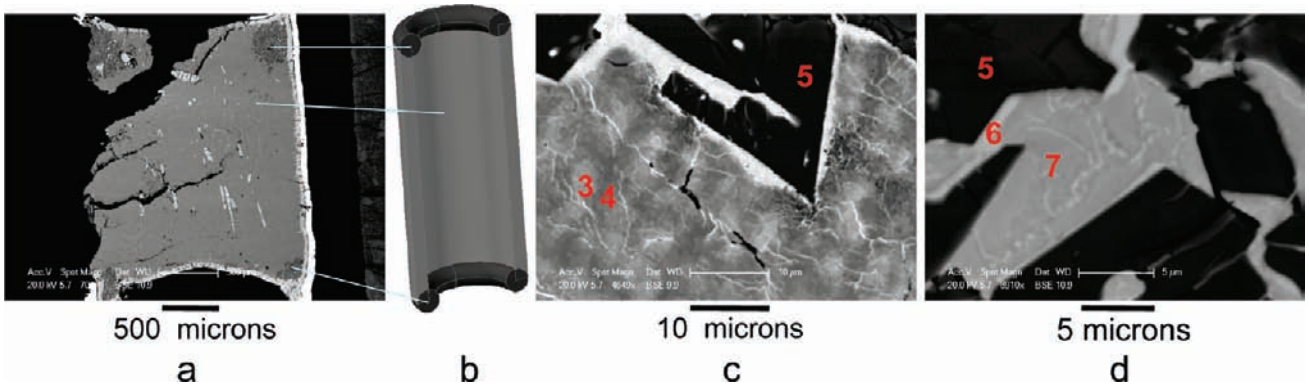

Figure 6. Lower (a) and higher (c, d) magnification SEM images in BSE mode of a polished section of the capsule of a Ge−Sn sample heated at 1500 K for 5 min at 9 GPa followed by annealing at 1000 K for 20 min, and followed then by temperature and pressure quenching. The higher magnification BSE image in (c) depicts both the bulk region quenched from the melt, and the cooler rim region annealed in the solid state. The higher magnification region in (d) depicts a part of the cooler rim section. (b) is a schematic of the half-capsule showing the bulk and cooler rim sections and the corresponding sections in the actual SEM images. Each of the two cooler rim sections, as seen, is actually a torus. Numerous EDX analyses from the seven regions of different contrast, as labeled in the figures, show that the brightest contrast rim region is the Re capsule (1), the somewhat lighter colored region is a Re−Ge phase (2), the dark and light contrast regions in the bulk of the capsule are Ge−Sn agglomerates, with the lighter contrast agglomerate (3) containing 15 at% less Ge than the darker contrast agglomerate (4). In the annealed sections, the darkest contrast region contains pure Ge (5) whereas the brightest contrast Ge−Sn region (6) (depletion zone) contains about 8 at% less Ge than the intermediate contrast region (7) in those sections (see also Supporting Information).

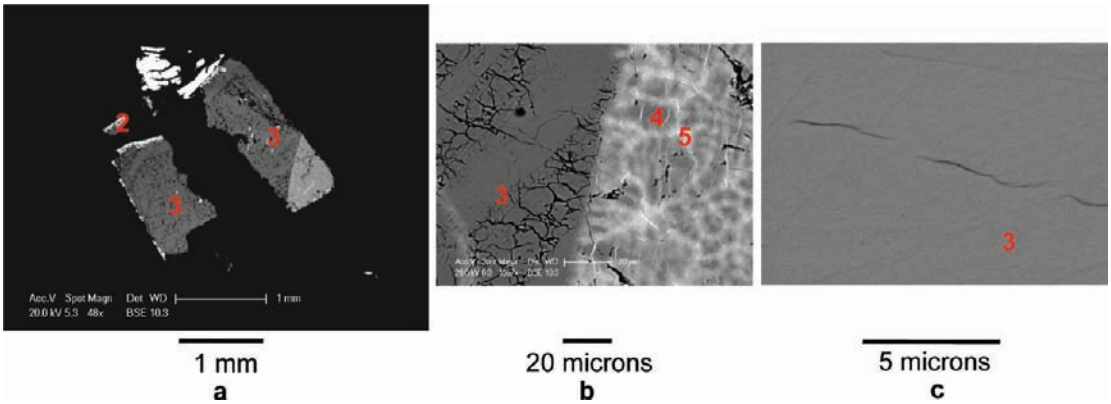

Figure 7. Lower (a) and higher (b) magnification SEM images in BSE mode of a polished section of a Ge−Sn sample heated at 1500 K at 10 GPa for 5 min followed by annealing at 770 K for 1 h before temperature and pressure quenching. The brighter triangular region shown in the lower right of the images in (a) and in (b) was quenched directly from the melt. Numerous EDX analyses from the five regions of different contrast, as labeled in the figure, show that the brightest contrast region is the Re capsule (1), the slightly lighter contrast regions are a Re−Ge phase (2), the extensive homogeneous regions is a uniform $Ge_{0.9}Sn_{0.1}$[1] phase (3), and the small triangular region on the right is composed of a mixture of darker contrast Ge-rich (4) (81 at% Ge) and lighter contrast Ge-poor (5) (39 at% Ge) agglomerates. (c) A higher resolution field emission gun scanning electron microscope image of (3) is also shown confirming the complete chemical homogeneity of the new $Ge_{0.9}Sn_{0.1}$ solid solution (see also Supporting Information).

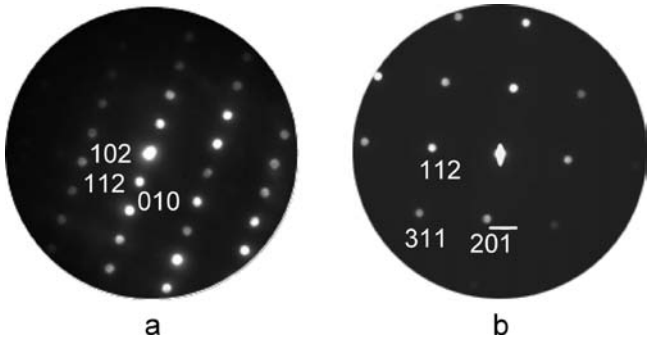

Figure 8. [−201] (a) and [−15−2] (b) zone-axis microdiffraction patterns of the tetragonal (S.G. $P4_32_12$) $Ge_{0.9}Sn_{0.1}$ structure.

than endmember tetragonal Ge. In 14 multianvil experiments above 10 GPa regardless of heat treatment protocol (see also Supporting Information), no such homogeneous region could be attained, Ge-rich and Sn-rich agglomerates were recovered, even though segregation into pure Ge regions and pure Sn regions was not achieved (Figure 9).

Discussion

We provide here an explanation for the detailed nature of the recovered products presented above. The structure and the metallic character of the Ge and Sn liquid states are considered to increasingly resemble each other with higher pressure.[11] To ~3 GPa however, the combination of the significant segregation tendency of the binary liquid state[25] and the distinctly dissimilar, structurally and electronically, solid states (Figure 1) means that segregation into pure Ge and Sn will easily take place upon cooling. Indeed, this is reflected by the sharp boundaries separating Ge from Sn directly quenched from the melt, that is, without the need for annealing (Figure 2). Between ~3 and 9 GPa the segregation tendency of the liquid state becomes less pronounced, while the Ge and Sn solid states still differ (Figure 1). Thus at 7 GPa segregation is not as facile as at lower pressures (Figure 3).

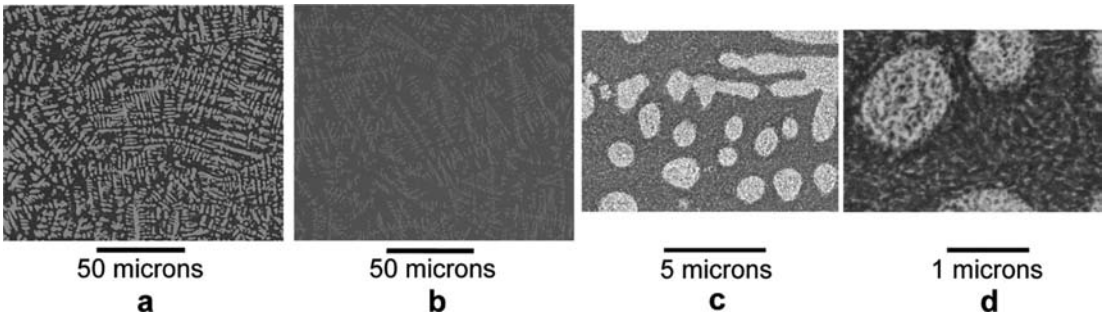

Figure 9. SEM images in BSE mode of polished sections of 2 Ge−Sn samples both heated at 1500 K at 24 GPa for 5 min followed respectively (a) by annealing at 1000 K for 10 min before temperature and pressure quenching and (b) by annealing at 1050 K for 5 h before temperature and pressure quenching. Numerous EDX analyses from the brighter and darker contrast regions in the two recovered products revealed Sn-rich and Ge-rich agglomerates, respectively. Annealing somewhat widens the domains of the Ge-rich and Sn-rich regions, but the data only support intimate agglomerates of Ge and Sn. (c, d) Higher resolution field emission gun scanning electron microscopy images of (b) are also shown confirming the extensive chemical heterogeneity of the recovered sample (see also Supporting Information).

While extensive pure Ge regions evolve, there are significant regions where segregation is not complete. That the process is moving toward segregation can be seen from the Sn-richer rim surrounding pure Ge, which shows that remaining Ge is still in the process of segregating from Sn after direct quenching from the melt. At 8 GPa, and further at 9 GPa, the segregation tendency of the liquid state decreases further, so that direct quenching from the melt no longer permits development of pure Ge regions, unless subsolidus annealing is undertaken, in which case segregation is facilitated (Figures 4−6). Indeed at 8 GPa the majority of the recovered product has been annealed in the solid state and, unlike the case at 7 GPa, sharp boundaries separate Ge from Sn (Figure 4). The absence of an intermediate Sn-rich composition adjacent to the Ge-rims signifies that segregation of Sn from Ge is largely complete. Contrastingly, the boundary between pure Ge and the residual melt-quenched liquid is depleted of Ge, showing that segregation of Ge from Sn in the quenched liquid is not complete (Figure 4). At 9 GPa segregation of Sn from Ge is even more difficult, as evidenced by the intimate mixture of Ge-rich and Sn-rich agglomerates in the recovered melt-quenched product (Figure 5). This increasing difficulty in separating Sn from Ge at 9 GPa, even as compared to proximal 7 or 8 GPa, as the segregation tendency of the liquid state decreases further, and the metallic character of the solid states converge, can be seen by the nature of the reaction products in a further experiment at 9 GPa where the sample was annealed at 1000 K after melting (Figure 6). This temperature is close to the liquidus,[5] and indeed the majority of the recovered product is quenched from the melt (Figure 6) and resembles the intimate mixture of Ge and Sn-rich agglomerates shown in Figure 5. The cooler upper and lower rims of the capsule, however, allow subsolidus annealing of the mixture near the rims, giving rise to pure Ge and a two phase Sn-rich region, with the area adjacent to pure Ge being Sn richer (Figure 6c). These observations again designate that segregation of the two components is not yet complete upon quenching from 1000 K (and from somewhat lower temperature near the rims), and that reaction between Ge and Sn is not favored at this pressure either. Near 10 GPa at lower temperatures, both the structural and electronic properties in the solid state satisfy the conditions for solid solution formation (Figure 1). Further, the liquid state segregation tendency is further decreased. Thus annealing, followed by cooling to room temperature facilitates reaction between Ge and Sn and solid solution formation, giving rise to a completely homogeneous recovered product (Figures 7, 8). The residual melt-quenched region, being a hotter, liquid region, was able to accommodate more Sn homogeneously with Ge in the liquid state. Upon quenching, the excess tin and the absence of annealing in this region, results in intimately mixed Sn-rich and Ge-rich regions. Above 10 GPa Ge-rich and Sn-rich agglomerates of varying extent were always recovered regardless of annealing time (Figure 9), because of the combination of a liquid state with diminished segregation tendency with respect to lower pressure, and ensuing metallic solid states for both Ge and Sn (Figure 1). The incompatibility however, of their atomic radii and crystal structures, make formation of a bulk crystalline Ge−Sn solid solution problematic.

Hence only near 10 GPa is formation of a bulk crystalline Ge−Sn phase favored. From the equilibrium phase stability point of view, the documented reason for this is that the structural and electronic criteria for solid solution between Ge and Sn are met near 10 GPa.[23] From the metastable phase stability point of view we suggest that there might be two further factors influencing solution of Sn in Ge near 10 GPa. The first factor may be linked to possible enhancement of reactivity in a region of profuse structural and electronic phase transitions, that is, a region in a state of flux. Namely, (i) at about 10 GPa, Ge is near a triple point,[5,7] (ii) in the solid state it transforms between semiconducting cubic Ge and the metallic β-tin structure, and (iii) Sn transforms between β-tin and a bct tetragonal phase. Thus this region of pronounced reconstruction and reformation might be more conducive to reaction between Ge and Sn. The second factor may be linked to the low liquid diffusivity near the low-lying triple point near 10 GPa. Low liquid diffusivity namely promotes formation of a bulk homogeneous structurally disordered system (elemental Ge-glass)[38,39] upon rapid cooling. Here, upon cooling of a lower segregation tendency, with respect to lower pressures, Ge−Sn liquid, the slow liquid diffusivity on the precipice of solidification, may also partly deter the two elements from separating, so that they retain random ordering in the same solid phase as well, which upon annealing results in formation of the bulk positionally disordered but structurally ordered system (i.e., crystalline Ge−Sn solid solution).

(38) Bhat, M. H.; Molinero, V.; Soignard, E.; Solomon, V. C.; Sastry, S.; Yarger, J. L.; Angell, C. A. *Nature* **2007**, *448*, 787–791.
(39) Molinero, V.; Srikanth, S.; Angell, C. A. *Phys. Rev. Lett.* **2006**, *97*, 075701–075704.

Considering the present experimental results and their analysis in their totality, as well as first X-ray diffraction measurements,[40] we put forth a broader perspective on the solid state (i) equilibrium and (ii) metastable phase relations within the extended pressure and temperature regime examined here. The equilibrium phase diagram of bulk Ge−Sn between ambient and 24 GPa consists of virtually pure Ge and pure Sn at all pressures and temperatures except in a narrow region near 10 GPa where a bulk crystalline $Ge_{0.9}Sn_{0.1}$ is stable together with any excess Sn. The metastable phase diagram like the equilibrium phase diagram also consists of virtually pure Ge and Sn between ambient and up to between 3.5 and less than 7 GPa. Between 7 and 9 GPa, as well as above 10 to 24 GPa, Ge-rich nanocrystals together with pure Sn may coexist, but with the Ge-rich nanocrystals not able to grow in size and sinter into a bulk crystalline Ge−Sn phase without dissociating into Ge and Sn, analogous to the behavior observed in likewise metastable Ge−Sn thin films.[41,42] The content of Ge in the nano-Ge-rich phase can vary depending on pressure, temperature, and quenching conditions. Near 10 GPa the metastable phase diagram, like the equilibrium phase diagram, consists of a bulk extended $Ge_{0.9}Sn_{0.1}$ crystalline phase together with any excess Sn, and depending on exact annealing and quenching conditions it may be possible to incorporate some additional Sn in the Ge−Sn crystalline phase. An amorphous Ge-rich phase may also be recoverable from between about 7 and 24 GPa depending on heating and quenching profile.

Conclusions

From a hierarchical materials design viewpoint, this work documents directly how modification of the underlying electronic (continuum description) and atomistic structures (nm to μm) is correlated with the resulting microstructure (μm to mm).[43] As such these results also provide a testbed for predictive computer-aided materials design across different length-scales.[44] Further, this direct imaging approach in conjunction with structural investigation is particularly powerful in revealing kinetic versus thermodynamic effects influencing the nature of the recovered products and their stability, by identifying detailed compositional variations (e.g., depletion zones) as well as product differentiation as a function of temperature gradients and possibly density driven separation. The thermodynamic and kinetic aspects of phase relations can then in turn be exploited in concert for preparing new materials. Also, the work provides a window into what should increasingly become a versatile approach for examining in situ and ex-situ the evolution of reactions under extreme conditions, namely, highest possible resolution 3-D profiling of chemical, structural, and morphological changes[45] as a function of variables including pressure, temperature, and time.

Acknowledgment. High-pressure experiments were performed at the Bayerisches Geoinstitut under the EU "Research Infrastructures: Transnational Access" Programme (Contract No. 505320 (RITA) − High Pressure). The TEM facility in Lille (France) is supported by the Conseil Regional du Nord-Pas de Calais and the European Regional Development Fund (ERDF). We also acknowledge the use of the EPSRC Chemical Database Service at Daresbury. We further warmly thank Ahmed Addad for his work and consultation on chemical microanalysis using scanning transmission electron microscopy, J. Craven for his assistance with scanning microscopy, M. Hall for demanding solids processing, S. Gourlay for assistance with schematic designs, and L. Nigay for critical readings of the manuscript.

Supporting Information Available: Tabulated description of experimental runs is found in Part I, compositional and morphological analyses in Part II, and definition of salient terminology in Part III. This material is available free of charge via the Internet at http://pubs.acs.org.

(40) Serghiou, G. et al., ongoing work.
(41) Ragan, R.; Guyer, J. E.; Meserole, E.; Goorsky, M. S.; Atwater, H. A. *Phys. Rev. B* **2006**, *73*, 235303–235314.
(42) Bratland, K. A.; Foo, Y. L.; Spila, T.; Seo, H. S.; Haasch, R. T.; Desjardins, P. *J. Appl. Phys.* **2005**, *97*, 044904–044913.
(43) Pettifor, D. G. *Phys. Educ.* **1997**, *32*, 164–168.
(44) Yip, S. *Nat. Mater.* **2003**, *2*, 3–5.
(45) Midgley, P. A.; Ward, E. P. W.; Hungria, A. B.; Thomas, J. M. *Chem. Soc. Rev.* **2007**, *36*, 1477–1494.